

Effects of morphology, conformation and configuration on the IR and Raman spectra of various poly(lactic acid)s

G. Kister, G. Cassanas* and M. Vert

CRBA, URA CNRS 1465, University Montpellier 1, Faculty of Pharmacy,
 15 Avenue Charles Flahault, 34060 Montpellier cedex, France
 (Revised 3 March 1997)

Morphology, conformation and configuration of a series of aliphatic polyesters of the polylactide-type were studied by ^{13}C n.m.r. and vibrational spectroscopies. Investigations were performed on the stereocomplex (PLAcomplex) formed by cocrystallisation of poly(L-lactic acid) and poly(D-lactic acid), on poly(D,L-lactic acid) and on poly(*meso*-lactide) stereocopolymers. Comparison was made with poly(L-lactic acid) PLA100, taken as a reference. Fundamental vibrations were correlated to bands characterising morphology, conformation and configuration of these different polymers. Factor group analysis based on the 10_3 and 3_1 helical conformations of semi-crystalline PLA100 and PLAcomplex, respectively, led to good agreement with information collected from X-ray diffraction. It was further shown that difference in tacticity between amorphous 'preferentially isotactic' poly(D,L-lactic acid) and 'preferentially syndiotactic' poly(*meso*-lactide) can be detected from the vibrational position of δCH and symmetric δCH_3 bending modes. Solid state ^{13}C n.m.r. confirmed the different conformations of semi-crystalline PLA100 and PLAcomplex, but did not allow us to discriminate the different tacticities of the amorphous stereocopolymers, contrary to Raman spectroscopy. © 1997 Elsevier Science Ltd.

(Keywords: poly(lactic acid); solid state ^{13}C n.m.r.; IR; Raman)

INTRODUCTION

Spectral techniques, especially ^{13}C n.m.r. and vibrational spectroscopies (IR and Raman) are powerful tools for the study of polymer structures¹. So far, high resolution ^1H and ^{13}C n.m.r. spectroscopies were primarily used to determine the stereoregularity of polymers in solutions. However, Raman and IR spectra are also sources of information to qualitatively and quantitatively evaluate other characteristics², namely: (i) extent of conformational and configurational isomerisms from band frequency assignments; (ii) degree and nature of crystalline and non-crystalline order from the intensities of the assigned bands; (iii) nature of chain folding from mixed crystal IR and Raman studies. Raman scattering provides well resolved spectra of vibrational fundamental modes. It does not affect the historical morphology of the sample. Molecular symmetry analysis is possible thanks to the complementary nature of IR and Raman data whose activities obey selection rules governing the vibrational energy levels³.

The family of aliphatic polymers derived from lactide stereomers (LA) and other lactones, especially glycolide (GA) and ϵ -caprolactone (CL), is currently considered as a source of bioresorbable biomaterials for temporary therapeutic applications⁴, namely suture materials, bone fracture internal fixation devices in surgery⁵, and drug delivery system in pharmacology⁶. The biological and physical properties of these materials are strongly related to the chemical structure of repeating units and to macromolecular characteristics such as chiral unit distribution, crystallinity and tacticity. Degradation kinetics depend on these

characteristics too. It is therefore worthwhile to identify the chemical and morphological structures of polymers in the solid state by techniques requiring no specific preparation which can always affect the history of samples.

Lactic acid-based aliphatic polyesters can be synthesised from various monomers. Low molecular weight polymers are obtained by step-growth polymerisation of lactic acid, whereas high molecular weight polymers are synthesised by ring-opening polymerisation of lactide. Lactide is composed of two lactic acid units linked to form a diester cyclic monomer. Both lactic acid and lactide are chiral. There are two lactic acid enantiomers and four different lactides. Indeed, the lactide cycle bears two identical asymmetric carbon atoms in L-lactide, D-lactide, and D,L-lactide which is a 50/50 mixture of L- and D-lactides, or two different ones in *meso*-lactide. PLA_X is the acronym used to represent homopolymers and stereocopolymers of lactic acid where X is the percentage of L-lactyl units. In a PLA_X stereocopolymer chain, the distribution of chiral repeating units can differ very much, depending on the synthesis route and on the feed. Step growth polymerisation of optically pure L-lactic acid (or pure D-lactic acid) and ring-opening polymerisation of optically pure L-lactide (or pure D-lactide) should lead to the same isotactic chain structure, provided no racemisation occurs during chain growth. Actually, dramatic differences in main chain structures are observed as soon as one deals with stereocopolymers composed of L- and D-lactic acid repeating units. The step growth polymerisation of mixtures of L- and D-lactic acid leads to poly(D,L-lactic acid) or PLA50a with a random distribution of the L- and D-lactyl units, whereas ring-opening polymerisation of the lactide dimers leads to non-random distributions because chains grow through a

* To whom correspondence should be addressed

pair addition mechanism⁷⁻⁹. Racemic D,L-lactide yields poly(D,L-lactic acid) or PLA50i, subscript i standing for predominantly isotactic because of the predominance of *iso*-dyads (L,L or D,D pairs) sequences over L,D or D,L *hetero*-dyads. Poly(*meso*-lactide) or PLA50s obtained from *meso*-lactide is predominantly syndiotactic because of the predominance of *hetero*-dyads (L,D or D,L pairs)⁹. Another lactic acid-based compound is a highly crystalline material (PLAcomplex)¹⁰ which is formed by PLA100 poly(L-lactic acid) and PLA0 poly(D-lactic acid) stereocomplexation. Stereocomplexation was also observed for stereocopolymers with complementary blocky structures¹¹. PLAX and PLAcomplex present different macroscopic solid state morphologies, depending on the composition in chiral units. PLA50's are amorphous, whereas PLA100 (or PLA0) and PLAcomplex, are highly semi-crystalline with helical conformations.

In the present study, we wish to report solid state ¹³C n.m.r., Raman and IR spectra of the different homopolymer, stereocopolymers and stereocomplex of lactides at room temperature. Furthermore, the spectra of the PLA stereocopolymers and of the stereocomplex were discussed in terms of morphology, conformation, and configuration on the basis of a complete assignment of vibrational fundamental frequencies which are typical of semi-crystalline PLA100.

EXPERIMENTAL

Materials

PLA100 was obtained by bulk ring-opening polymerisation of L-lactide at 145°C using zinc powder as the initiator. Low molecular weight residual compounds were removed by the dissolution-precipitation method with acetone/methanol as solvent/precipitant. The precipitated powder was compression moulded (200 bars) as plates and then machined as parallel side specimens according to the usual process¹². Quenched poly(L-lactic acid), PLA100am, was recovered from the cooled mould, whereas semi-crystalline PLA100 was obtained after annealing of PLA100am specimens in an oven at 130°C for 2 hr. The degree of crystallinity was nearly 73%, as deduced from X-ray diffractometry. Relative weight average molecular weights ($\overline{M}_w \approx 100,000$) were determined by size-exclusion chromatography as referred to polystyrene standards.

PLA50i resulted from the polymerisation of D,L-lactide at 145°C using zinc powder as the initiator¹². Low molecular weight residual compounds were removed by dissolution in acetone and precipitation with methanol. The recovered polymer was vacuum-dried for 1 week and compression moulded as round plates.

PLA50s was obtained from *meso*-lactide in the presence of Zn metal at 145°C. PLA50a resulted from the polycondensation of D,L-lactic acid at 145°C. Poly(L-lactic acid)/poly(D-lactic acid) stereocomplex, or PLAcomplex, was prepared according to the procedure used by Tsuji *et al.*¹³. Poly(L-lactic acid) and poly(D-lactic acid) were dissolved simultaneously in acetonitrile (0.25%) at 82°C. The solution was kept at the same temperature for 1 week. The precipitates were separated by filtration and extracted with the solvent to remove the uncomplexed polymer fraction. Finally, the stereocomplex was vacuum-dried for 1 week.

X-ray diffraction

X-ray diffraction spectra were recorded on a diffractometer equipped with a CuK α ($\lambda = 0.155$ nm) source, a monochromator and a CGR goniometric plate.

¹³C n.m.r. spectra

High-resolution solid-state ¹³C n.m.r. spectra were carried out on a Bruker AM300 spectrometer operating at 75.470 MHz. For CP/MAS spectra, the contact time was 5 msec and the recycle times were 5 sec. For MAS without cross polarisation, a 90° pulse of 4–8 μ sec for carbon was used. All the spectra were recorded at room temperature.

Raman spectra

Raman spectra were obtained with a Jobin-Yvon HG2S spectrometer. The 514.5 nm line of the Spectra Physics 2017 argon ion laser was used as excitation source. Laser power was 100 mW. Scanning operations and data processing were controlled by a spectralink board and an IBM PC computer. The integration time was 1 sec with a scanning increment of 1 cm⁻¹ and a bandwidth of 2 cm⁻¹. PLA(s) were analysed as fragments of polymeric samples, without specific preparation. Spectra were recorded at room temperature after the exposure time necessary to decay the fluorescence.

Band deconvolution to separate the multiple components observed was carried out using a commercial package *Spectra Calc* purchased from Galactic Industries. The band shape used was a mixture of Gaussian and Lorentz functions. This program provides the capability to fix, if necessary, any parameter used to describe the band position, shape, or intensity. Relative intensity was then measured as the integrated area of individual deconvoluted peaks.

Infrared spectra

IR spectra were recorded on a Perkin Elmer 983G spectrometer. Thin films were cast from chloroform solutions onto a KRS5 plate.

RESULTS AND DISCUSSION

X-ray diffraction

The morphology of the various PLA selected for this study was first checked by X-ray diffraction (*Figure 1*). These patterns exhibited well-defined bands for PLA100 and for PLAcomplex. The observed peaks ($\theta = 8.3^\circ, 9.5^\circ$ for PLA100 and $\theta = 6.0^\circ, 10.35^\circ, 12.0^\circ$ for PLAcomplex) well agreed with the characteristics of 10₃ (α -form) and 3₁ helices, respectively, as mentioned in Ref. 14. The broad diffusion band observed in the spectra of quenched PLA100am and various PLA50's were typical of amorphous polymeric compounds.

¹³C n.m.r. spectroscopy

Solid state ¹³C n.m.r. chemical shifts were obtained through dipolar decoupling (DD), magic angle spinning (MAS) and cross-polarisation (CP) technique¹⁵. *Figure 2* shows the solid-state ¹³C CP/MAS spectra obtained for all the PLA polymers at room temperature and with a contact time of 5 ms. Amorphous PLA100am, PLA50i, PLA50a and PLA50s presented identical spectra characterised by broad resonance lines at 16.9, 69.4 and 170.0 ppm corresponding to methyl, methine and carbonyl carbon atoms, respectively. MAS without CP and with high dipolar decoupling showed the same behavior at room temperature, and thus did not allow us to differentiate the various amorphous compounds. In contrast, the spectra of semi-crystalline PLA100 and PLAcomplex were different. Each resonance line exhibited splittings or dissymmetric bands. In particular, the carbonyl carbon resonance was split into three peaks (169.9, 171.0, 172.0 ppm) in PLA100. In

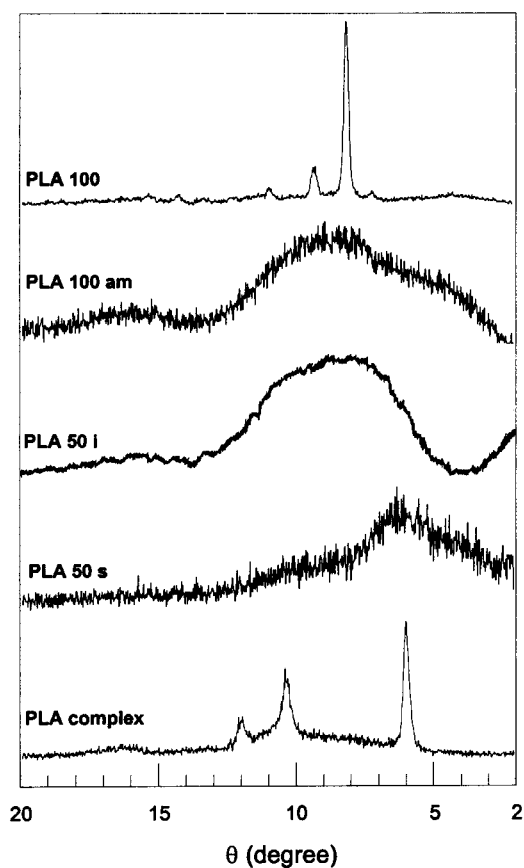


Figure 1 X-ray diffractograms of poly(L-lactic acid): PLA100 (semi-crystalline), PLA100am (amorphous), PLA50i (isotactic), PLA50s (syndiotactic) and PLAComplex (stereocomplex)

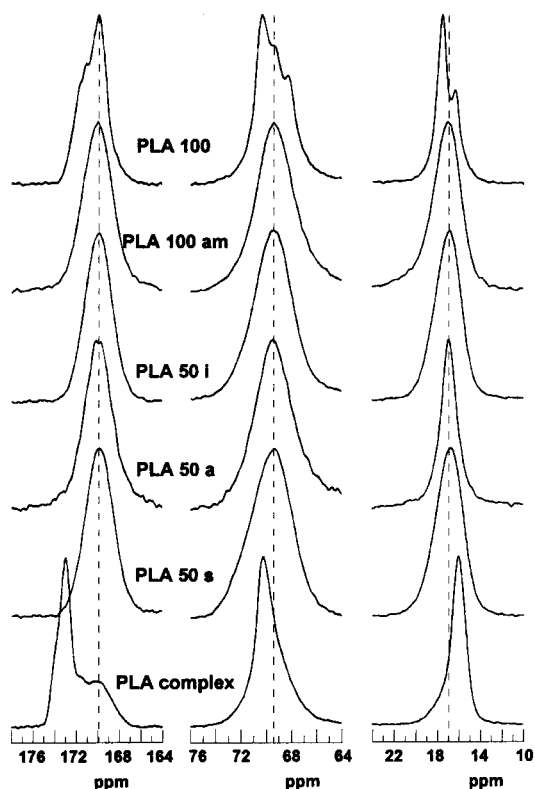


Figure 2 CP/MAS ^{13}C spectra of poly(L-lactic acid): PLA100 (semi-crystalline), PLA100am (amorphous), PLA50i (isotactic), PLA50a (atactic), PLA50s (syndiotactic) and PLAComplex (stereocomplex)

PLAcomplex, the same carbon atom line could be decomposed into an intense peak at 173 ppm with a shoulder at 174 ppm and two other bands at 170 and 171 ppm. The two latter bands were considered as reflecting the non-crystalline and crystalline microdomains present in crystallised PLA100 or PLA0 homopolymers¹⁶. Three methine signals (68.2, 69.3 and 70.3 ppm) and two methyl signals (16.4 and 17.5 ppm) were observed for PLA100. In contrast, PLAcomplex spectra showed one dissymmetric line for each CH and CH₃ carbon type, with a maximum at 70.2 ppm and at 16.1 ppm, respectively. These differences could be generated by corresponding solid state helical conformations shown by X-ray diffraction (*Figure 1*). In PLA100, splittings of resonance lines also reflected a different crystalline packing in the chains within the lattice. Besides the 173 ppm peak, the multiple component lines observed in PLAcomplex can arise from the presence of amorphous domains and of homopolymer residues.

IR and Raman analysis

Figures 3 and 4 present the IR and Raman spectra of the various PLA polymers. Comparison was made by spectral regions with previous data obtained for PLA100¹⁷ and for L and DL-lactic acids and corresponding oligomers^{18,19}. *Table 1* shows the PLA100 IR and Raman frequencies which were used as references.

Morphology-conformation

Figure 4 shows that only the Raman spectra of PLA100 and of the stereocomplex exhibited sharp lines. These lines seemed to result from splittings of the lines which appeared

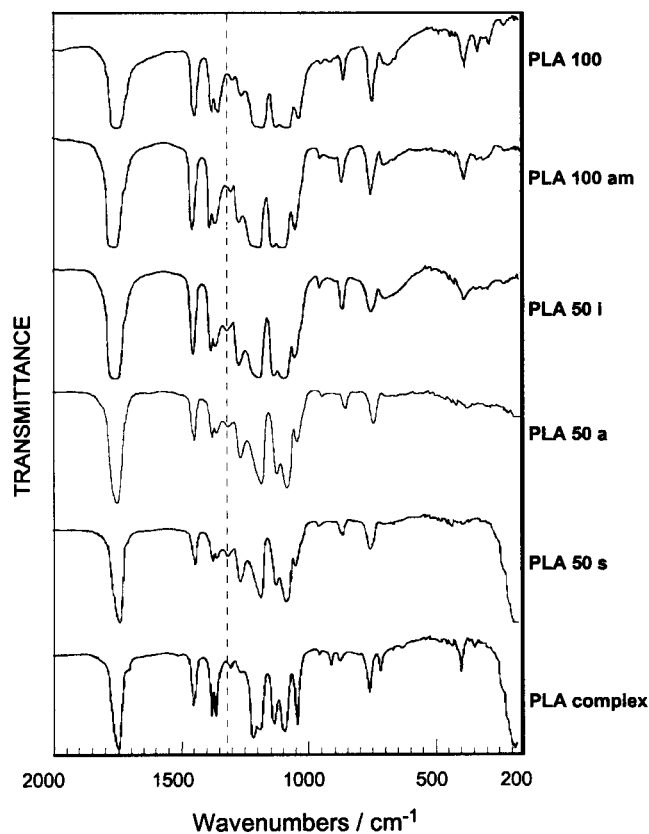


Figure 3 Infrared spectra of poly(L-lactic acid): PLA100 (semi-crystalline), PLA100am (amorphous), PLA50i (isotactic), PLA50a (atactic), PLA50s (syndiotactic) and PLAComplex (stereocomplex) - - - - : band sensitive to the tacticity

Table 1 Wavenumbers (cm^{-1}) and vibrational assignments of semi-crystalline PLA100 Poly(L-lactic acid)

Raman ν/cm^{-1}	IR ν/cm^{-1}	Assignments
3014 M–3000 sh–2995 S	2997 M	$\nu_{\text{as}}\text{CH}_3$
2970 sh		$\nu_{\text{as}}\text{CH}_3$
2960 sh		$\nu_{\text{as}}\text{CH}_3$
2943 VS	2947 M	$\nu_{\text{s}}\text{CH}_3$
2901 w–2877 M	2882 w	νCH
1773 S–1763 S–1769 sh–1749 S	1760 VS	$\nu\text{C}=\text{O}$
1452 S	1452 S	$\delta_{\text{as}}\text{CH}_3$
1394 sh–1388 M–1382 sh	1348–1388 S	$\delta_{\text{s}}\text{CH}_3$
1371 M–1366 M–1353 M	1368 S–1360 S	$\delta_1\text{CH} + \delta_2\text{CH}_3$
1313 sh–1302 M–1293 M	1315–1300 M	$\delta_2\text{CH}$
1270 w	1270 S	$\delta\text{CH} + \nu\text{COC}$
1216 w–1179 w	1215 VS–1185 VS	$\nu_{\text{as}}\text{COC} + \nu_{\text{as}}\text{CH}_3$
1128 S	1130 S	$\nu_{\text{as}}\text{CH}_3$
1092 S–1088 sh	1100 VS–1090 sh	$\nu_{\text{s}}\text{COC}$
1050 sh–1042 S	1045 S	$\nu\text{C}-\text{CH}_3$
954 vw–920 M	960 w–925 w	$\nu\text{CH}_3 + \nu\text{CC}$
873 VS–845 w	875 M–860 sh	$\nu\text{C}-\text{COO}$
760 sh–736 M	760 S–740 sh	$\delta\text{C}=\text{O}$
711 M–677 sh–650 sh	715 M–695 M	$\gamma\text{C}=\text{O}$
578 w–520 M	515 w	$\delta_1\text{C}-\text{CH}_3 + \delta\text{CCO}$
411 S–398 S	415 sh–400 M	δCCO
347 w	350 M	$\delta_2\text{C}-\text{CH}_3 + \delta\text{COC}$
325 sh–308 S–300 w	300 M–295 sh	$\delta\text{COC} + \delta_2\text{C}-\text{CH}_3$
251 w–234 w	240 M	τCC
218 w–206 w		τCC
160 S		skeletal torsion
117 S		skeletal torsion
77 S		skeletal torsion
60 M		skeletal torsion

VS = very strong; S = strong; M = medium; w = weak; sh = shoulder; s = symmetric; as = asymmetric.

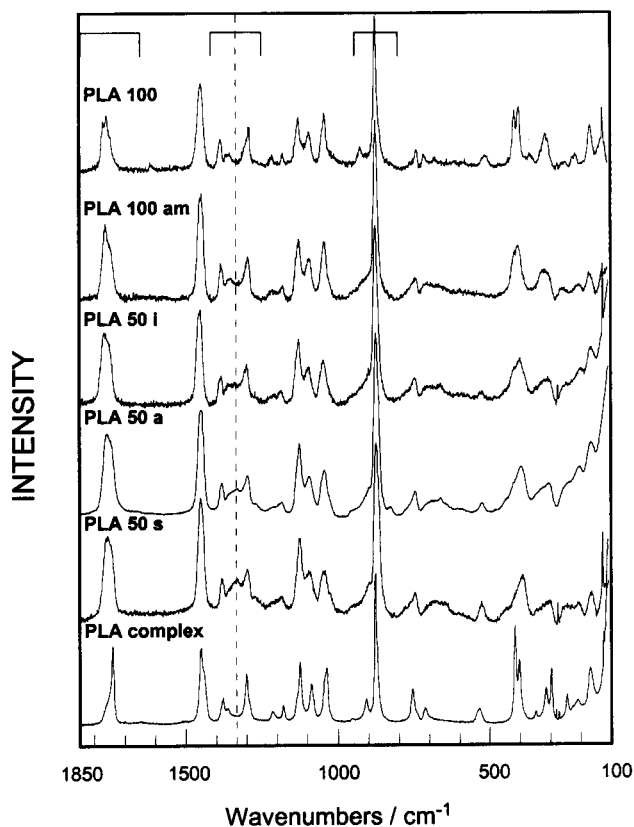
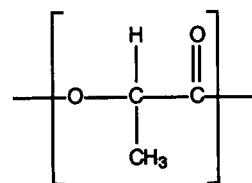


Figure 4 Raman spectra of poly(L-lactic acid)s: PLA100 (semi-crystalline), PLA100am (amorphous), PLA50i (isotactic), PLA50a (atactic), PLA50s (syndiotactic) and PLAcxplex (stereocomplex). — — —: band sensitive to the tacticity; \square : zones expanded in figures 5–8

broad in the spectra of the amorphous compounds. This sharpness agreed well with the presence of crystalline domains in PLA100 and PLAcxplex, whereas the broad lines formed in the spectra of PLA50 stereocopolymers reflected amorphous compounds. Spectral differences were observed between semi-crystalline compounds corresponding to the two helical conformations. In the α -form, PLA100 crystallises in a hexagonal or pseudo-orthorhombic system with two chains per unit cell, each one in a left-handed helical 10_3 conformation (ten physical repeat units in three turns)²⁰. The triclinic unit cell of PLAcxplex involved poly(L-lactide) and poly(D-lactide) chains in 3_1 helical conformation (three monomers per turn), with left-handed helical PLA100 chain and right-handed helical PLA0 chain alternatively side by side²¹. Factor group analysis was applied to semi-crystalline α -form PLA100 and to PLAcxplex. The analysis was based on the vibrational theory of polymers¹⁵.

In the PLA100 α -form, 10_3 helix contains $N = 90$ atoms in the translational repeat unit. The factor group of line group is $C(6\pi/10)$ isomorphous with the cyclic group C_{10} which contains ten symmetry elements (E identity and nine screw C_{10}^k axes).



Using group theory, the nine atoms of the chemical unit give rise to 270 ($= 3N$) normal vibrations. Among them four are non-genuine and result from pure translations of the chain and from rotation around the chain axis:

$$\Gamma_{\text{vib}} = 25A + 27B + 26E_1 + 27(E_2 + E_3 + E_4)$$

$$\Gamma_{\text{rot-trans}} = 2A + E_1$$

In the vibrational modes of A symmetry, all physical repeating units vibrate in phase when related by the screw operation. In the modes of B symmetry, alternate units vibrate π -out of phase. The E_m species correspond to modes of doubly degenerate pairs vibrating at the same frequency, with a phase angle of $\pm 6\pi m/10$ between consecutive units around an axis parallel to the helical axis. Using the selection rules¹⁵, E_3 and E_4 modes are IR and Raman inactive. A, B, E_1 and E_2 are Raman active, whereas only A and E_1 modes are IR active.

In PLA complex, each translational repeat unit of the 3_1 helix is formed of 27 atoms. The factor group of the line group is isomorphous with the point group C_3 giving rise to $3N - 4 = 77$ genuine vibrations, classified as:

$$\Gamma_{\text{vib}} = 25A + 26E$$

where A and E modes are IR and Raman active, E modes being doubly degenerate pairs.

In the case of PLA50 compounds which were amorphous, the absence of crystalline phases caused a broadening of lines in the IR and Raman spectra.

C=O stretching region. Figure 5 presents the 1650–1850 cm^{-1} region of the Raman spectra. In PLA100, the Raman line assigned to $\nu\text{C}=\text{O}$ stretching mode was split into components corresponding to A, B, E_1 and E_2 species modes. These modes were observed at 1749, 1763, 1769 and 1773 cm^{-1} . In the IR spectrum, the A and E_1 active modes overlapped to give a broad asymmetric band at about

1760 cm^{-1} . In the spectrum of PLA100am, the Raman lines were broad and asymmetric and the deconvolution analysis showed two components at 1768 (S) and 1749 (M) cm^{-1} certainly due to the pair addition mechanisms¹⁹. These two latter bands were also present in the PL50 stereocopolymers, showing perturbation in helical chain structure caused by the introduction of D,D or D,L units. The spectrum of the stereocomplex was simpler than that of PLA100 and showed a sharp peak at 1745 cm^{-1} and a 1760–1780 cm^{-1} broad diffusion band. The line with the strongest intensity was assignable to the A-type mode and corresponded to the totally symmetric vibration, whereas the large diffusion line could be decomposed into the E mode peak and a band relative to the amorphous component.

In PLA(s), the C=O stretching mode is consequently sensitive to the morphology and the conformation. The double bands observed at 1768 and 1749 cm^{-1} for amorphous compounds were considered as resulting from the particular chiral unit enchainments generated by the pair addition mechanism which governs the LA ring opening polymerisation.

CH₃ and CH bending region. The CH₃ asymmetric deformation modes appeared at about $1450 \pm 2 \text{ cm}^{-1}$ as intense Raman and IR bands in all the compounds. Their stability in frequency reflected a pure vibrational mode (Figure 4).

Figure 6 presents the 1250–1400 cm^{-1} region of the Raman spectra. Like in polypropylene²² and poly(α -L-alanine)²³, this region was characterised by three groups of bands at ≈ 1390 , ≈ 1360 and $\approx 1300 \text{ cm}^{-1}$. In PLA100, corresponding deconvolution suggested overlapped splittings corresponding to A, B, E_1 and E_2 modes with maxima

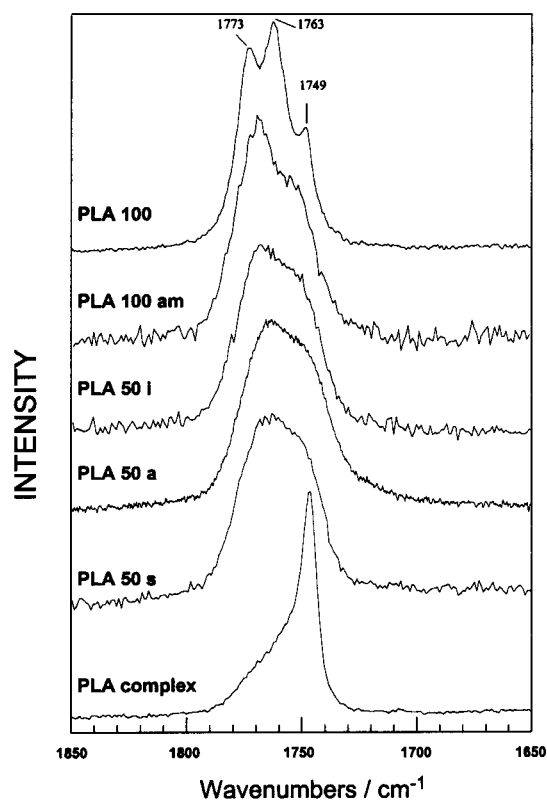


Figure 5 Raman spectra (1650–1850 cm^{-1} region) of poly(L-lactic acid)s: PLA100 (semi-crystalline), PLA100am (amorphous), PLA50i (isotactic), PLA50a (atactic), PLA50s (syndiotactic) and PLA complex (stereocomplex)

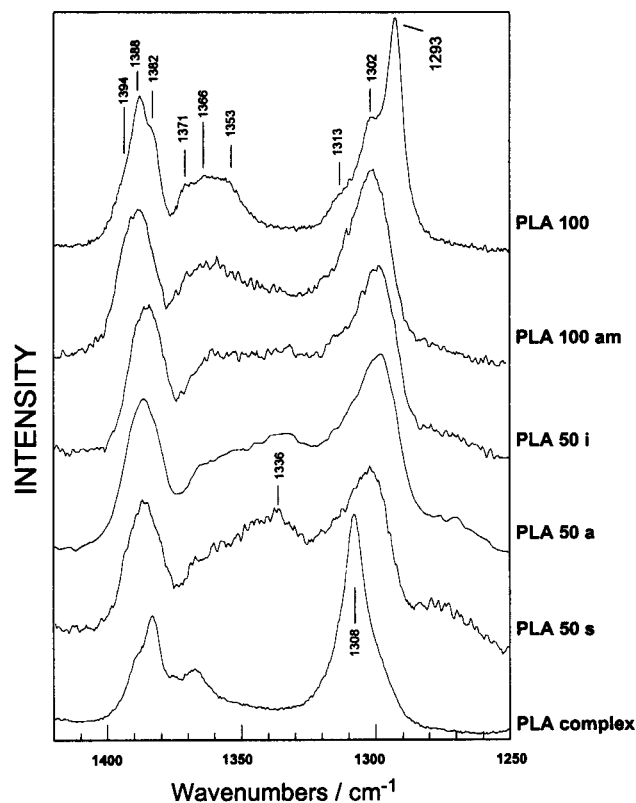


Figure 6 Raman spectra (1250–1420 cm^{-1} region) of poly(L-lactic acid)s: PLA100 (semi-crystalline), PLA100am, (amorphous), PLA50i (isotactic), PLA50a (atactic), PLA50s (syndiotactic) and PLA complex (stereocomplex)

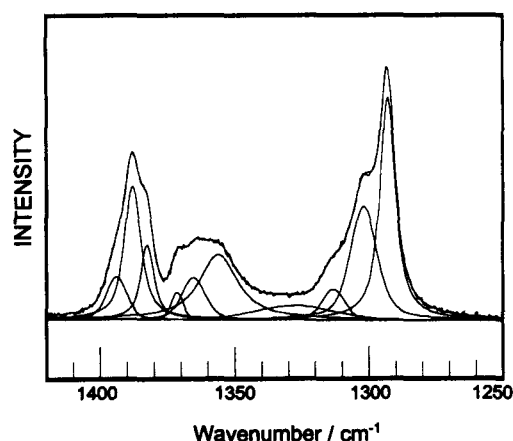


Figure 7 Raman spectra of semi-crystalline PLA100 in the 1250–1420 cm^{-1} : deconvolution analysis

at 1382–1388–1394 cm^{-1} , 1353–1366–1371 cm^{-1} and 1293–1302–1313 cm^{-1} (Figure 7). In PLAcomplex, doublets including A and E modes were found at 1382–1389 cm^{-1} , 1366–1374 cm^{-1} and 1298–1308 cm^{-1} . These splittings characterise the semi-crystalline state of PLA100 and PLAcomplex. It is of value to note that quenching PLA100 to PLA100am suppressed the sharp peaks and the band splittings due to crystallinity. These peaks were replaced by broad asymmetric lines deconvoluted into two components attributed to the (L,L) unit pairing as in the C=O stretching region. For amorphous PLA50 stereocopolymers, the first and the third groups of bands appeared broad in Raman spectra and showed frequency minor shifts and similar intensities. They were assigned to the $\delta_s\text{CH}_3$ symmetric deformation and the δCH bendings, respectively.

Skeletal stretching and $r\text{CH}_3$ rocking region. Figure 3 shows several strong absorption bands in the 1000–1250 cm^{-1} region. The 1185 and 1215 cm^{-1} doublet observed in PLA100 could be assigned to symmetric C–O–C stretching modes (A and E_1 types) of ester groups. Asymmetric C–O–C modes were observed at 1090 cm^{-1} as a disymmetric IR band. The corresponding Raman lines were of low intensity. Two other bands appeared near 1130 and 1045 cm^{-1} in the Raman and IR spectra. They were also found in lactic acid oligomers¹⁸ at the same frequency and were assigned to $r\text{CH}_3$ rocking and $\nu\text{C}-\text{CH}_3$ stretching, respectively.

The enlarged 800–950 cm^{-1} region is presented in Figure 8. In all the Raman spectra, the most intense line was located at ca. 870 cm^{-1} . It was assigned to $\nu\text{C}-\text{COO}$ stretching, as shown by spectral changes during L-lactic acid polycondensation¹⁹. This line becomes asymmetric in PLA50's. For the PLAcomplex, the corresponding peak appeared at 880 cm^{-1} . A second Raman line of medium intensity was observed at 920 and 908 cm^{-1} in the spectra of PLA100 and PLAcomplex, respectively, and was absent in the amorphous compounds. The first band reflected the 10_3 helix, whereas the second one reflected the 3_1 helix. They were assigned to the coupling of the $\nu\text{C}-\text{C}$ backbone stretching with CH_3 rocking mode, as in polypropylene and poly(α -L-alanine)^{24–26}. The presence of this medium line depends on both the crystallinity of the polymer and the type of helical conformation.

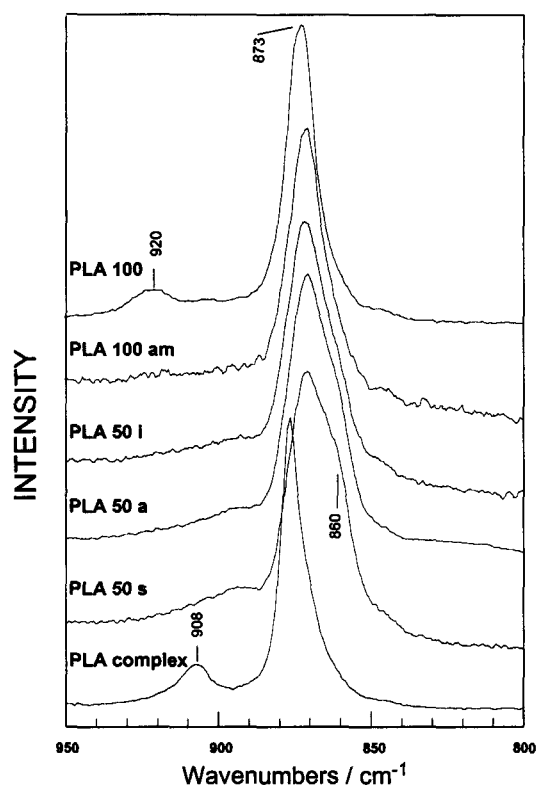


Figure 8 Raman spectra (800–950 cm^{-1} region) of poly(L-lactic acid)s: PLA100 (semi-crystalline), PLA100am (amorphous), PLA50i (isotactic), PLA50a (atactic), PLA50s (syndiotactic) and PLAcomplex (stereocomplex)

Low frequency region. The $\delta\text{C}=\text{O}$ and $\gamma\text{C}=\text{O}$ modes of PLA100 were observed at 736–760 cm^{-1} and at 650–677–711 cm^{-1} , respectively in Raman spectra (Figure 4). As compared with the other spectra, the PLAcomplex lines were sharper and located at slightly higher frequencies. Below 600 cm^{-1} , the Raman lines were more sensitive to modifications of chain morphology²⁴. The spectra of semi-crystalline PLA100 and PLAcomplex showed splittings of deformation vibrations which are composed of bendings and torsions. The 398–411 cm^{-1} doublet in PLA100 and PLAcomplex spectra were assigned to δCCO mode. Only a broad line was observed in amorphous stereocopolymers. For PLAcomplex, the δCOC skeletal chain deformations appeared as split lines at lower frequencies (291–309 cm^{-1}). The bands at around 230, 210 and 160 cm^{-1} for PLA100 and at 239, 206 and 160 cm^{-1} for PLAcomplex were characteristic of torsion modes.

Configuration

The presence of D- and L-lactyl units in PLA50 and the mechanisms of lactic acid polycondensation and of lactide ring opening polymerisation led to different configurational structures, namely PLA50a, PLA50i, PLA50s as recalled in the Introduction. Spectra seemed to depend on these configurational structures.

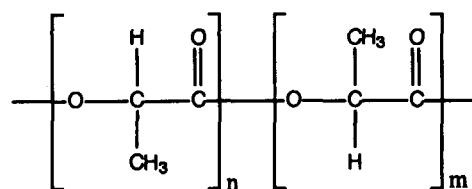


Figure 5 presents the $\nu_{C=O}$ region. The intensity of the shoulder at 1749 cm^{-1} increased with the degree of syndiotacticity of polymer.

The most important change occurred in the $1310\text{--}1360\text{ cm}^{-1}$ region corresponding to $\delta_s\text{CH}_3$ and δCH modes (Figure 6). As compared with PLA100, the presence of D-LA units in the chain led to the appearance of a weak and broad Raman line at 1336 cm^{-1} of stronger intensity in the spectrum of the preferentially syndiotactic PLA50s. A new absorption band was observed at 1320 cm^{-1} . These two bands are now considered as specific of the syndiotactic character of poly(meso-lactide) or PLA50s and can be used to discriminate PLA50i and PLA50s.

The backbone ν_{CC} also presented configuration dependent line shapes. Figure 8 shows the 873 cm^{-1} Raman line observed for PLA100 which became asymmetric in PLA50s. The intensity of the shoulder located at about 860 cm^{-1} increased when going from PLA50i to PLA50s.

CONCLUSION

Comparison was made of solid state X-ray diffraction, ^{13}C n.m.r. and vibrational (IR and Raman) spectra of various lactic acid-derived polymers. Solid state ^{13}C n.m.r. did not allow us to distinguish the specific unit distribution present in the various amorphous PLA50. However, it showed different magnetic environments for semi-crystalline PLA100 and PLACOMPLEX in agreement with the two different helical arrangements typical of these polymers. Solid state ^{13}C n.m.r. appeared as a limited technique to provide information on the morphology of PLA polymers. A new series of CP/MAS ^{13}C magnetic relaxation behavior experiments will be useful to estimate the optimal contact time for various mobility phases and thus to allow enhanced discrimination of the tacticities.

Raman and IR spectra appeared as more sensitive to molecular arrangement. They allowed us to distinguish 10_3 and 3_1 helical conformations of PLA100 and PLACOMPLEX, respectively. Moreover, they allowed us to discriminate the different amorphous PLA50, namely the preferentially isotactic, the preferentially syndiotactic and the atactic ones, based on the frequency shifts and the intensities of the δCH and $\delta_s\text{CH}_3$ bendings corresponding lines. Further work is under way in an attempt to find out simple spectroscopic investigations capable of identifying both the chemical nature and the morphology of solid state PLA_XGA_Y and PLA_XCL_Y copolymers derived from L- or D, L-lactide and glycolide (GA) or ϵ -caprolactone (CL).

REFERENCES

1. Koenig, J. L., *Spectroscopy of Polymers*, ACS Professional Reference Book, American Chemical Society, Washington DC, 1992.
2. Bower, D. I. and Maddams, W. F., *The Vibrational Spectroscopy Of Polymers*, Cambridge Solid State Sciences Series, Cambridge University Press, 1989.
3. Painter, P. C., Coleman, M. M. and Koenig, J. L., in *The Theory of Vibrational Spectroscopy and its Application to Polymeric Materials—2*, John Wiley and Sons, New York, 1982, p. 238.
4. Li, S. and Vert, M., in *Degradable Polymers*, ed. G. Scott and D. Gilead, Chapman and Hall, London, 1995.
5. Schindler, A., Jeffcoat, R., Kimmel, G. L., Pitt, C. G., Wall, M. E. and Zweidinger, R., in *Contemporary Topics in Polymer Sc—2*, ed. E. M. Pearce and J. R. Schaefgen, Plenum Press, New York, 1977, p. 251.
6. Domb, A. J., Amselem, S., Maniar, M., in *Polymeric Biomaterials—1*, ed. S. Dumitriu, M. Dekker Inc, New York, 1994, p. 399.
7. Lillie, E. and Schulz, R. C., *Makromol. Chem.*, 1901, **1975**, 176.
8. Schindler, A., *Polym. Letters*, 1976, **14**, 729.
9. Chabot, F., Vert, M., Chapelle, S. and Granger, P., *Polymer*, 1983, **24**, 53.
10. Ikada, Y., Jamshidi, K., Tsuji, H. and Hyon, S.-H., *Macromolecules*, 1987, **20**, 904.
11. Wisniewski, M., *Synthese de stereocopolymeres de l'acide lactique par polymerisation de lactides avec differents alcoolates metalliques*, Thesis, Univ. Montpellier I, France, 1995.
12. Leray, J. and Vert, M., *Blanquaert French Patent Application*, 76-28163, 1976.
13. Tsuji, H., Hyon, S.-H. and Ikada, Y., *Macromolecules*, 1992, **25**, 2940.
14. Brizzolara, D., Cantow, H.-J., Diederichs, K., Keller, E. and Domb, A. J., *Macromolecules*, 1996, **29**, 191.
15. Bovey, F. A., *Chain Structure and Conformation of Macromolecules*, Academic Press, London, 1982.
16. Tsuji, H., Horii, F., Nakagawa, M., Ikada, Y., Odani, H. and Kitamaru, R., *Macromolecules*, 1992, **25**, 4114.
17. Kister, G., Cassanas, G., Vert, M., Pauvert, B. and Térol, A., *J. Raman Spectrosc.*, 1995, **26**, 307.
18. Kister, G., Cassanas, G., Fabrègue, E. and Bardet, L., *Eur. Polym. J.*, 1992, **28**, 1273.
19. Cassanas, G., Kister, G., Fabrègue, E., Morssli, M. and Bardet, L., *Spectrochim. Acta Part A*, 1993, **49**, 271.
20. De Santis, P. and Kovacs, A. J., *Biopolymers*, 1968, **6**, 299.
21. Okihara, T., Tsuji, M., Kawagushi, A., Katayama, K.-I., Tsuji, H., Hyon, S.-H. and Ikada, Y., *J. Macromol. Sci. -Phys.*, 1991, **B30**(1 and 2), 119.
22. Painter, P. C., Coleman, M. M. and Koenig, J. L., in *The Theory of Vibrational Spectroscopy and its Application to Polymeric Materials—3*, John Wiley and Sons, New York, 1982, p. 377.
23. Rabolt, J. F., Moore, W. H. and Krimm, S., *Macromolecules*, 1977, **10**, 1065.
24. Itoh, K. and Shimanouchi, T., *Biopolymers*, 1970, **9**, 383.
25. Dwivedi, A. M. and Krimm, S., *Biopolymers*, 1984, **23**, 923.
26. Frushour, B. G. and Koenig, J. L., *Biopolymers*, 1975, **14**, 363.